

PRETRAINED CONFORMERS FOR AUDIO FINGERPRINTING AND RETRIEVAL

Kemal Altlwanky^{1,2}, Elmedin Selmanovic², Sead Delalic²

¹Infobip

²University of Sarajevo

ABSTRACT

Conformers have shown great results in speech processing due to their ability to capture both local and global interactions. In this work, we utilize a self-supervised contrastive learning framework to train conformer-based encoders that are capable of generating unique embeddings for small segments of audio, generalizing well to previously unseen data. We achieve state-of-the-art results for audio retrieval tasks while using only 3 seconds of audio to generate embeddings. Our models are almost completely immune to temporal misalignments and achieve state-of-the-art results in cases of other audio distortions such as noise, reverb or extreme temporal stretching. Code and models are made publicly available and the results are easy to reproduce as we train and test using popular and freely available datasets of different sizes.

Index Terms— audio fingerprinting, audio retrieval, conformer, contrastive learning, self-supervised learning

1. INTRODUCTION

Given a small excerpt of an audio, the task of content-based audio retrieval is to identify the original audio from which the excerpt was taken. Content-based audio retrieval is often performed using audio fingerprinting techniques; for every audio file of interest, a unique fingerprint is generated by taking smaller segments of the audio and generating low-dimensional representations of the segments. These low-dimensional representations collectively make up the audio fingerprint. Retrieval using an excerpt is performed by computing the low-dimensional representations of the excerpt and finding corresponding matches, often facilitated through vector search. Retrieval is limited to audio files for which fingerprints have been made and added to a database, while extending the database is performed by simply updating it with new fingerprints. Note that these low-dimensional representations do not necessarily need to be embeddings (or more generally vectors), instead, they can be as simple as pairs of time-frequency coordinates within the spectrogram, as is usually the case in more classical audio fingerprinting approaches.

The most common application of audio fingerprinting is in music identification services, such as those offered by Apple (Shazam) [1], Google (Now Playing [2]), SoundHound [3] and others. Audio fingerprinting is also used for detecting copyright infringements or tracking advertisements [1, 4]. In telecommunications, audio fingerprinting has been employed to search for duplicate audio when identifying unsolicited phone calls [5, 6] or even improve network performance by quickly identifying announcements played during session initiation [7, 8].

In [9] the authors classify audio fingerprinting techniques into three categories: local descriptors-based [10, 11, 12], peak-based

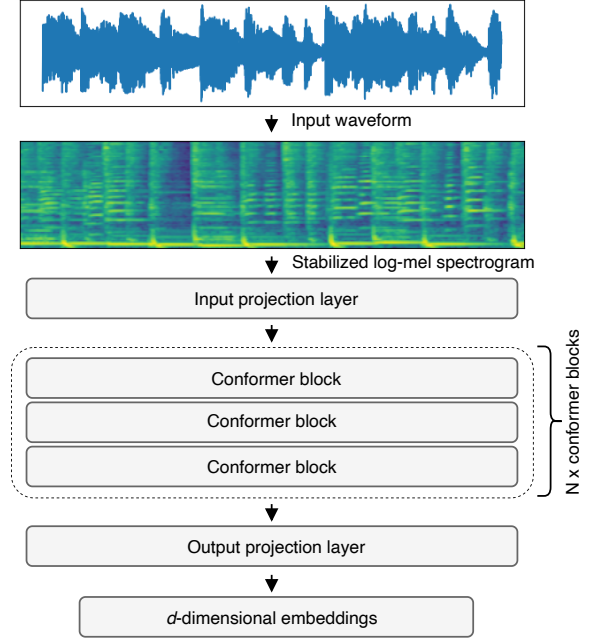


Fig. 1. Encoder architecture. We compute the stabilized log-mel spectrogram and pass it through a linear projection layer, followed by several (N) conformer blocks, before a final projection layer that outputs d -dimensional embeddings.

[1, 13, 14] and neural-based approaches [2, 4, 15]. Neural-based approaches are mainly based on contrastive learning frameworks and convolutional neural networks (CNNs) [2, 4]. Recent advances such as PeakNetFP [9] combine peak extraction techniques with contrastive learning. GraFPrint [16] is the first approach to utilize Graph Neural Networks (GNNs), while the authors of [17] demonstrate an attention-based approach.

Our contributions can be summarized as follows; we propose the first conformer-based architecture for neural audio fingerprinting, achieving state-of-the-art results for audio retrieval tasks. CNNs exploit local features effectively, while transformers are good at capturing content-based global interactions and have achieved state-of-the-art results in speech recognition [18, 19]. Conformers combine the best of both worlds, which makes them a suitable choice for audio fingerprinting tasks; when recognizing audio, the spectral content itself is just as important as its positioning in time within the audio. After an initial pretraining phase, our models learn to general-

ize well and can generate unique embeddings for previously unseen data. This paper is accompanied by three open source models and code which enables easy replication of our results. We highlight the importance of data augmentation during training, especially the task of generating difficult contrastive examples to prevent the models from overfitting.

2. METHOD

Figure 1 provides a high-level overview of our proposed conformer-based architecture.

2.1. Conformer encoder

We present three models, which are limited by the number of their parameters: small (1.5M), medium (8.8M) and large (26.2M). The model architectures, spectral parameters and hyperparameters are summarized in Table 1. All of our encoders share the high-level architecture from Figure 1; they compute the stabilized log-mel spectrogram from an input audio waveform and propagate it through the network. The output is a d -dimensional embedding, which is ℓ_2 normalized. All models were trained using the Adam optimizer [20] (default values; $\beta_1 = 0.9$, $\beta_2 = 0.999$, $\epsilon = 1e-8$) and a dropout rate $P_{drop} = 0.5$. The learning rate was kept constant for the small and medium models, while a simple hybrid adaptive strategy was applied that gradually decreased the learning rate while increasing the batch size during training of the large model.

2.2. Contrastive learning

Similar to previous work [2, 4, 9, 16], we use the SimCLR self-supervised contrastive learning framework [21] in which we wish to minimize the normalized temperature-scaled cross entropy loss (NT-Xent). The training process is visualized in Figure 2. Given a mini-batch of B audio segments (samples), we generate a replica for each of the B samples by applying various audio augmentation techniques. The original z_i and replica z_j are considered positive pairs, while the remaining $2(B-1)$ samples are all treated as negative examples. In literature, $\text{sim}(z_i, z_j) = z_i^\top z_j / \|z_i\| \|z_j\|$ is commonly used to denote the cosine similarity between two samples z_i and z_j , which is equal to the dot product in our case, as we ℓ_2 normalize the embeddings at the output of our model. The loss for a positive pair of samples (i, j) is computed as:

$$\ell_{i,j} = -\log \frac{\exp(\text{sim}(z_i, z_j)/\tau)}{\sum_{k=1}^{2B} \mathbb{1}_{[k \neq i]} \exp(\text{sim}(z_i, z_j)/\tau)} \quad (1)$$

where $\mathbb{1}_{[k \neq i]} \in \{0, 1\}$ evaluates to 1 iff $k \neq i$ and τ is the temperature parameter. The loss is now computed for each positive pair, both (i, j) and (j, i) , and averaged into the total cost function. The training process is illustrated in Figure 2.

2.3. Data

Our models are trained using the Free Music Archive (FMA) [22]. FMA provides predefined subsets, categorized as small (8k tracks), medium (25k tracks), and large (106k tracks), with each subset already split into train-test-validation splits. Perhaps unconventionally, but we decided to train the small (1.5M), medium (8.8M) and large (26.2M) models using the small (8k), medium (25k) and large (106k) subsets of FMA, respectively. This choice was deliberate, as we wanted to make the small/medium models easier to reproduce. Although downsizing the models with fewer layers and parameters

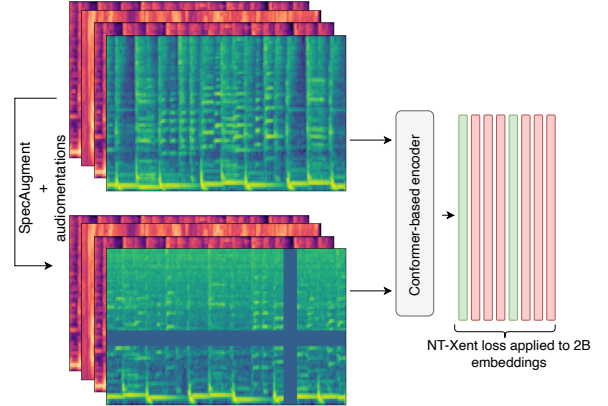


Fig. 2. Training process. For a B -sized mini-batch, we augment each sample and pass the original and augmented versions through our encoder resulting in a total of $2B$ embeddings. We compute the NT-Xent loss by treating the original and its derived augmented replica as positive pairs, whereas the remaining $2(B-1)$ samples are treated as negatives. The bottom green spectrogram is an augmented version of the top one, it is temporally shifted to the left, it’s spectral content is pitch shifted (upward), it contains blue noise and some frequencies and time points have been masked.

achieves this to some degree, a large dataset can still pose challenges for scientists lacking high-performance computing resources.

2.4. Generating positive pairs

As shown in Figure 2, the self-supervised training process consists of selecting B samples from the training set and applying data augmentation techniques to generate replicas, whose distance in the embedding space we wish to minimize from the distance of the originals.

We rely on the Python audiomentations library [23] to augment data; adding background noise at various SNR rates (datasets ESC-50 [24] and MS-SNSD [25]), adding colored noise at various SNR and decay rates, applying impulse response/reverb (dataset MIT IR Survey [26]), pitch-shifting the audio, applying polarity inversion, applying tanh distortion, time-stretching the audio and time-shifting

Table 1. Model architecture, spectral and hyper-parameters.

Model	Small	Medium	Large
Num Params (M)	1.5	8.8	26.2
Encoder Dim	256	512	768
Encoder Layers	2	3	4
Attention heads	4	8	12
Conv kernel size	5	5	5
Embeddings dim	128	128	128
Sample rate	16k	16k	16k
Input len (sec)	3	3	3
FFT len	1024	1024	1024
Hop len	128	128	128
N mels	80	80	96
Training set (samples)	6.4k	20k	83k
Epochs	100	100	100
NT-Xent τ	0.07	0.05	0.05
Learning rate	1e-4	2e-4	variable
Batch size	64	64	variable
Weight decay (λ)	5e-4	5e-4	5e-4

the audio.

Despite using various audio augmentations, we report that SpecAugment [27] was crucial to prevent overfitting, especially for our large model.

2.4.1. Beta-distributed temporal shifting

The input to all models is a 3-second long audio segment, which means that during training we randomly select such a segment from each audio taken into the batch. For a sample rate of 16 kHz this amounts to a segment of 48 k samples.

In practice, it is desirable to allow for slight temporal mismatches when performing audio retrieval, i.e. the query segment does not have to be temporally aligned with the retrieved segment. Initially, we opted for a maximum of 5% mismatch (150 ms or 2400 samples), thus we would randomly shift the replica (augmented audio) during training between 0 and 2400 samples.

Although no overfitting occurred, i.e. no substantial deviations between training and test/validation recall, the initial retrieval rates of models trained under such circumstances for relatively large time shifts, e.g. 120 ms, were not satisfying.

After some investigation, similar to FaceNet [28], we concluded that it is important to train the model on what the authors refer to as *hard* examples. Thus, the training process was adjusted to encourage larger temporal shifts (i.e. harder examples) by sampling the time offset by which we shift audio from a beta distribution instead of a uniform distribution, as illustrated in Figure 3. Sampling from a beta distribution with parameters $\alpha = 8$ and $\beta = 2$ with the minimum and maximum offset values of 0 ms and 150 ms will on average apply an offset of 120 ms. We report that this small change was crucial to improving performance and making our models almost completely robust to any temporal misalignments ranging from 0 ms to 150 ms.

3. EXPERIMENTS

After training each model on its respective training dataset, we compute the embeddings for the large test dataset of FMA [22]. Faiss [29] is used to store and retrieve the embeddings. Results regarding retrieval time or analyses regarding different indexing mechanisms of Faiss are left out since: (1) our work mainly focused on developing a conformer-based model for generating audio fingerprints, not an end-to-end audio retrieval application, and (2), Faiss is almost a standard for retrieval of audio embeddings, so similar results can be expected as in other approaches which utilize Faiss [4, 9, 16].

Each result that is reported represents an average over 5 identical test runs. In a single test, we perform 5 queries for every audio file by selecting 5 linearly spaced 3-second long excerpts of each audio. As is commonly done in audio fingerprinting literature, we report on the top-1 and top-5 hit rate, often referred to as the *exact* and *near* matches or *accuracy*. For easier distinction, the top-5 hit rate will further be enlisted inside parentheses.

3.1. Performance of conformer models

Of all distortions, our models are most robust to temporal shifts, which is supported by maintaining near-perfect results in the presence of such distortions, especially in terms of the top-5 hit rate. In Table 2, we provide the hit rates achieved when applying temporal shifts, expressed as a percentage of half the distance from the next fingerprint (i.e. 300 ms). The models perform well on this type of

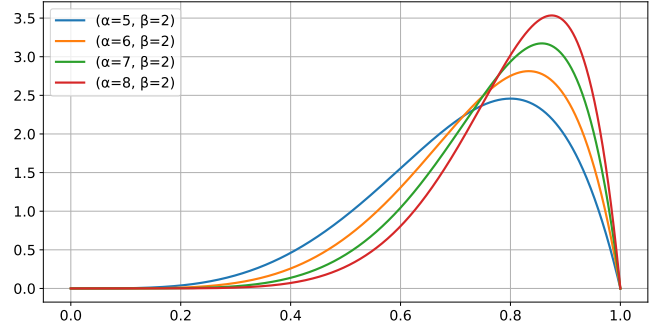


Fig. 3. Probability density function of the beta distribution for values $\beta = 2$ and $\alpha = [5, 6, 7, 8]$. Given $\alpha = 8$ and a maximum value of 150, the mean would amount to 120.

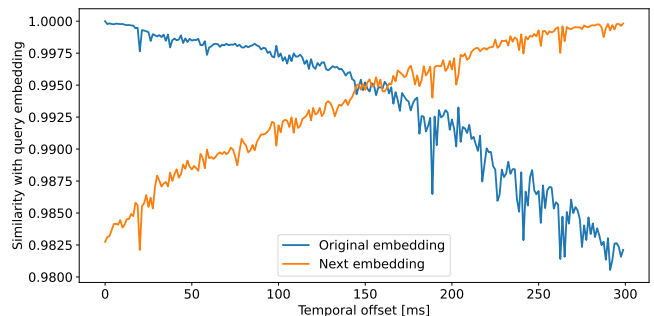


Fig. 4. Robustness to temporal shifts. For a given query embedding, we plot the similarity between itself (original) and the next embedding, which are spaced 300 ms apart. We gradually increase the temporal shift of the query (which now acts as a replica) and observe how the similarity between the replica and next embedding increases, while the similarity between the replica and original decreases. Note how the similarity curves intersect at around 150 ms.

distortion as they have learned to continuously decrease the similarity metric between two audio segments as the time distance between them increases, mimicking a monotonic function. Figure 4 illustrates this desirable property of the embeddings.

Table 2 provides the hit rates when dealing with reverb. Although these results are good, especially for the large conformer, the models are not as robust to reverb as to temporal offsets, which is further supported by Table 4 in which the overall performance for background and colored noises at various SNR levels is provided. Note that the results were evaluated using ESC-50 and the test split of MS-SNSD [24, 25], which none of the models has seen during training.

Table 2. Top-1 (top-5) hit rates for time-distorted queries.

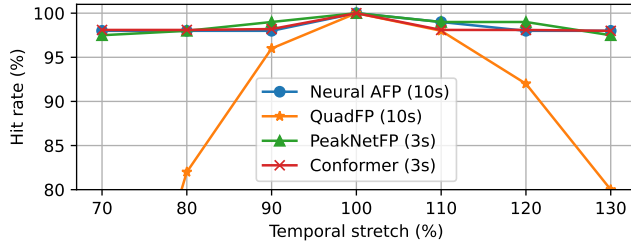
Model	Temporal shift (% of 300 ms)				Reverb
	10%	20%	30%	40%	
Small	98.7 (100)	98.8 (100)	98.5 (100)	98.4 (100)	88.8 (91.4)
Medium	98.6 (100)	98.6 (100)	98.4 (100)	98.3 (100)	92.2 (94.8)
Large	98.6 (100)	98.7 (100)	98.4 (100)	98.2 (100)	96.2 (98.2)

Table 3. Comparison of our large conformer model (26.2M) with other audio fingerprinting approaches: top-1 hit rate.

Model	Query length	Embeddings size	Batch size	FMA subset	Top-1 hit rate (SNR)				Comment
					5 dB	10 dB	15 dB	No noise	
Conformer (26.2M)	3	128	arbitrary	large	93.9	97.1	97.8	98.8	Up to 120 ms temporal shift
NAFP [4]	5	128	640	large	/	≥ 92	≥ 92	≥ 92	Varying SNR (0-10 dB) and reverb
Now-playing [2, 4]	5	64	unknown	large	/	≥ 79.8	≥ 79.8	≥ 79.8	Implemented by NAFP [4] under same conditions
Dejavu [4, 12]	6	/	/	small	/	/	/	69.6	Reported by NAFP [4]
Audfprint [17, 30]	3	/	/	medium	88.5	91.4	93.8	/	Implemented by Attention-based [17]
Audfprint [17, 30]	5	/	/	medium	89.4	91.5	94.2	/	Implemented by Attention-based [17]
NAFP [4, 17]	3	128	512	medium	88.5	91.4	93.8	/	Implemented by Attention-based [17]
Attention-based [17]	3	128	512	medium	92.9	94.6	95.5	/	/
Attention-based [17]	5	128	512	medium	93.9	94.7	96.8	/	/
FE+HT [15]	3	128 (16-quantized)	/	medium	90.8	95.5	96.3	/	Up to 50 ms temporal shift
GraFPrint [16]	1	128	256	large	61.8	71.6	83.8	/	/
GraFPrint [16]	3	128	256	medium	98.3	99.3	99.6	/	/
Attention-based [16, 17]	3	128	unknown	medium	88.4	92.6	95.2	/	Implemented and reported by GraFPrint [16]

Table 4. Top-1 (top-5) hit rates for noise-distorted queries.

Model	Background noise			Colored noise		
	SNR 5dB	SNR 10dB	SNR 15 dB	SNR 5 dB	SNR 10dB	SNR 15dB
Small	83.4 (86.2)	92.9 (95.0)	96.0 (97.9)	77.8 (81.0)	88.7 (91.3)	93.5 (95.8)
Medium	87.8 (90.6)	95.0 (97.1)	96.8 (98.8)	91.8 (94.4)	95.6 (97.8)	97.0 (99.0)
Large	93.9 (96.2)	97.1 (99.0)	97.8 (99.6)	95.6 (97.8)	97.3 (99.2)	97.9 (99.7)

**Fig. 5.** Top-1 hit rate vs. temporal stretch.

3.2. Comparison with other fingerprinting approaches

3.2.1. Temporal distortions

We compare the performance of our best model with the current state-of-the-art Neural audio fingerprinter (NAFP) [4] and PeakNetFP [9] for time-stretching. These models can handle extreme audio slowdowns or speed-ups and have improved significantly compared to the previous state-of-the-art QuadFP [14]. Our model seems to perform very slightly under the performance of PeakNetFP at 90% and 110% time stretching, but it is marginally better at the more extreme rates of 70% and 130%, as shown in Figure 5. Note that QuadFP and NAFP use a query sample that is more than 3 times longer compared to PeakNetFP and the conformer.

3.2.2. Noise distortions

In Table 3, we compare the performance of our best model with the current state-of-the-art approaches in noisy conditions. It is difficult to discern and point out a clear winner, since there are many variables at play, e.g. the used length of the query sample, the size of the embeddings or the subset of FMA [22]. The audio distortions are also not uniform, in NAFP [4] the results were reported under a varying SNR range, whereas in [15, 16, 17] independent test runs were repeated by fixing these values. The most important differences are listed under column *Comments* inside Table 3.

3.3. Discussion

For noisy audio, GraFPrint [16] claims to achieve the best results with a given query length of only 3 seconds, evaluated on the medium subset of FMA. NAFP is the most tested and cited implementation and has been confirmed to achieve similar results by several sources [4, 9, 16, 17]. Aside being evaluated on the large subset of FMA, another advantage of NAFP is that it achieves state-of-the-art performance in cases of extreme time stretching, while GraFPrint does not report on the results for such distortions.

Given the results from Table 3 and Figure 5, we conclude that our large conformer model (26.2M) matches the current state-of-the-art in terms of extreme temporal distortions (NAFP [4], PeakNetFP [9]) using a small query length of 3 seconds. Regarding noisy distortions, the large model has comparable performance to the state-of-the-art (GraFPrint [16]), especially at SNR rates of 10 dB and 15 dB, while being the best performing model evaluated on the large subset of FMA [22]. Thus, our model achieves good results on both frontiers.

From Table 2 and Table 4, we conclude that the small (1.5M) and medium (8.8M) models do not exhibit state-of-the-art performance, except for temporal shifts. However, given their reduced size and complexity, these models are very suitable for applications in which no severe audio distortions are expected, being marginally outperformed by the large model in such circumstances.

4. CONCLUSION

Conformers excel at capturing both local and global interactions, making them a natural candidate for audio fingerprinting techniques. We showed that pretrained conformer encoders are capable of generating distinct embeddings for small segments of previously unseen audio which remain robust even in cases of severe audio distortions. Our best performing model matches the current state-of-the-art, while our smaller models achieve good results under lighter distortions. In future work, we aim to investigate quantization techniques, both on the encoder weights, as well as the embeddings generated by the encoder and to provide a framework for easier comparison and verification of audio fingerprinting techniques.

5. REFERENCES

- [1] Avery Wang et al., “An industrial strength audio search algorithm,” in *Proc. of the Int. Society for Music Information Retrieval (ISMIR)*, 2003, vol. 2003, pp. 7–13.
- [2] Beat Gfeller, Ruiqi Guo, Kevin Kilgour, Sanjiv Kumar, James Lyon, Julian Odell, Marvin Ritter, Dominik Roblek, Matthew

- Sharifi, Mihajlo Velimirović, et al., “Now playing: Continuous low-power music recognition,” in *NeurIPS 2017 Workshop on Machine Learning on the Phone and other Consumer Devices*, 2017.
- [3] SoundHound, “Discover, Search and Play Any Song by Using Just Your Voice,” <https://www.soundhound.com/soundhound/>, 2025, [Online; accessed 29-July-2025].
 - [4] Sungkyun Chang, Donmoon Lee, Jeongsoo Park, Hyungui Lim, Kyogu Lee, Karam Ko, and Yoonchang Han, “Neural audio fingerprint for high-specific audio retrieval based on contrastive learning,” in *IEEE International Conference on Acoustics, Speech and Signal Processing (ICASSP 2021)*. IEEE, 2021, pp. 3025–3029.
 - [5] Sathvik Prasad, Elijah Bouma-Sims, Athishay Kiran Mylappan, and Bradley Reaves, “Who’s calling? characterizing robocalls through audio and metadata analysis,” in *29th USENIX Security Symposium (USENIX Security 20)*, 2020, pp. 397–414.
 - [6] Daniel PW Ellis, Brian Whitman, and Alastair Porter, “Echoprint - an open music identification service,” in *Proc. of the Int. Society for Music Information Retrieval (ISMIR)*, 2011, vol. 2011, pp. 52–58.
 - [7] Kemal Altlwky, Hadžem Hadžić, Amar Kurić, and Emanuel Lacic, “Knowledge distillation for real-time classification of early media in voice communications,” in *2024 32nd International Conference on Modeling, Analysis and Simulation of Computer and Telecommunication Systems (MASCOTS)*. IEEE, 2024, pp. 1–4.
 - [8] Kosta Pribic, Sead Delalic, Hadzem Hadzic, Kemal Altlwky, Amar Kuric, Luka Cizmek, and Ivan Dumlija, “Systems and methods for media analysis for call state detection,” May 8 2025, US Patent App. 18/501,134.
 - [9] Guillem Cortès-Sebastià, Benjamin Martin, Emilio Molina, Xavier Serra, and Romain Hennequin, “Peaknetfp: Peak-based neural audio fingerprinting robust to extreme time stretching,” *arXiv preprint arXiv:2506.21086*, 2025.
 - [10] Jaap Haitsma and Ton Kalker, “A highly robust audio fingerprinting system,” in *Proc. of the Int. Society for Music Information Retrieval (ISMIR)*, 2002, vol. 2002, pp. 107–115.
 - [11] Michele Covell and Shumeet Baluja, “Known-audio detection using waveprint: Spectrogram fingerprinting by wavelet hashing,” in *2007 IEEE International Conference on Acoustics, Speech and Signal Processing-ICASSP’07*. IEEE, 2007, vol. 1, pp. I–237.
 - [12] Will Drevo, “Dejavu: audio fingerprinting and recognition algorithm,” <https://pypi.org/project/PyDejavu/>, 2014, [Online; accessed 01-August-2025].
 - [13] Six Joren and Marc Leman, “Panako-a scalable acoustic fingerprinting system handling time-scale and pitch modification,” in *Proc. of the Int. Society for Music Information Retrieval (ISMIR)*, 2014, vol. 2014, pp. 259–264.
 - [14] Reinhard Sonnleitner and Gerhard Widmer, “Robust quad-based audio fingerprinting,” *IEEE/ACM Transactions on Audio, Speech, and Language Processing*, vol. 24, no. 3, pp. 409–421, 2015.
 - [15] Anup Singh, Kris Demuynck, and Vipul Arora, “Simultaneously learning robust audio embeddings and balanced hash codes for query-by-example,” in *ICASSP 2023-2023 IEEE International Conference on Acoustics, Speech and Signal Processing (ICASSP)*. IEEE, 2023, pp. 1–5.
 - [16] Aditya Bhattacharjee, Shubhr Singh, and Emmanouil Benetos, “Grafprint: A gnn-based approach for audio identification,” in *ICASSP 2025-2025 IEEE International Conference on Acoustics, Speech and Signal Processing (ICASSP)*. IEEE, 2025, pp. 1–5.
 - [17] Anup Singh, Kris Demuynck, and Vipul Arora, “Attention-based audio embeddings for query-by-example,” in *Proc. of the Int. Society for Music Information Retrieval (ISMIR)*, 2022, vol. 2022, pp. 52–58.
 - [18] Anmol Gulati, James Qin, Chung-Cheng Chiu, Niki Parmar, Yu Zhang, Jiahui Yu, Wei Han, Shibo Wang, Zhengdong Zhang, Yonghui Wu, and Ruoming Pang, “Conformer: Convolution-augmented transformer for speech recognition,” in *Interspeech 2020*, 2020, pp. 5036–5040.
 - [19] Saidul Islam, Hanae Elmekki, Ahmed Elsebai, Jamal Bentahar, Nagat Drawel, Gaith Rjoub, and Witold Pedrycz, “A comprehensive survey on applications of transformers for deep learning tasks,” *Expert Systems with Applications*, vol. 241, pp. 122666, 2024.
 - [20] Diederik P Kingma and Jimmy Ba, “Adam: A method for stochastic optimization,” *arXiv preprint arXiv:1412.6980*, 2014.
 - [21] Ting Chen, Simon Kornblith, Mohammad Norouzi, and Geoffrey Hinton, “A simple framework for contrastive learning of visual representations,” in *International conference on machine learning*. PmlR, 2020, pp. 1597–1607.
 - [22] Michaël Defferrard, Kirell Benzi, Pierre Vandergheynst, and Xavier Bresson, “Fma: A dataset for music analysis,” in *Proc. of the Int. Society for Music Information Retrieval (ISMIR)*, 2017, vol. 2017, pp. 316–323.
 - [23] Iver Jordal, “iver56/audiomentations: v0.42.0,” Zenodo, 2025, doi: 10.5281/zenodo.15806235.
 - [24] Karol J Piczak, “Esc: Dataset for environmental sound classification,” in *Proceedings of the 23rd ACM international conference on Multimedia*, 2015, pp. 1015–1018.
 - [25] Chandan K.A. Reddy, Ebrahim Beyrami, Jamie Pool, Ross Cutler, Sriram Srinivasan, and Johannes Gehrke, “A scalable noisy speech dataset and online subjective test framework,” in *Interspeech 2019*, 2019, pp. 1816–1820.
 - [26] James Traer and Josh H McDermott, “Statistics of natural reverberation enable perceptual separation of sound and space,” *Proceedings of the National Academy of Sciences*, vol. 113, no. 48, pp. E7856–E7865, 2016.
 - [27] Daniel S. Park, William Chan, Yu Zhang, Chung-Cheng Chiu, Barret Zoph, Ekin D. Cubuk, and Quoc V. Le, “SpecAugment: A simple data augmentation method for automatic speech recognition,” in *Interspeech 2019*, 2019, pp. 2613–2617.
 - [28] Florian Schroff, Dmitry Kalenichenko, and James Philbin, “Facenet: A unified embedding for face recognition and clustering,” in *Proceedings of the IEEE conference on computer vision and pattern recognition*, 2015, pp. 815–823.
 - [29] Jeff Johnson, Matthijs Douze, and Hervé Jégou, “Billion-scale similarity search with GPUs,” *IEEE Transactions on Big Data*, vol. 7, no. 3, pp. 535–547, 2019.
 - [30] Daniel Ellis, “The 2014 labrosa audio fingerprint system,” in *ISMIR*, 2014.